

CONF-9705119--

LATTICE-MATCHED EPITAXIAL GaInAsSb/ GaSb  
THERMOPHOTOVOLTAIC DEVICES

G. Charache, C. A. Wang, et. al.

May 1997

DISTRIBUTION OF THIS DOCUMENT IS UNLIMITED

MASTER

NOTICE

This report was prepared as an account of work sponsored by the United States Government. Neither the United States, nor the United States Department of Energy, nor any of their employees, nor any of their contractors, subcontractors, or their employees, makes any warranty, express or implied, or assumes any legal liability or responsibility for the accuracy, completeness or usefulness of any information, apparatus, product or process disclosed, or represents that its use would not infringe privately owned rights.

KAPL ATOMIC POWER LABORATORY

SCHENECTADY, NEW YORK 10701

Operated for the U. S. Department of Energy  
by KAPL, Inc. a Lockheed Martin company

## **DISCLAIMER**

This report was prepared as an account of work sponsored by an agency of the United States Government. Neither the United States Government nor any agency thereof, nor any of their employees, makes any warranty, express or implied, or assumes any legal liability or responsibility for the accuracy, completeness, or usefulness of any information, apparatus, product, or process disclosed, or represents that its use would not infringe privately owned rights. Reference herein to any specific commercial product, process, or service by trade name, trademark, manufacturer, or otherwise does not necessarily constitute or imply its endorsement, recommendation, or favoring by the United States Government or any agency thereof. The views and opinions of authors expressed herein do not necessarily state or reflect those of the United States Government or any agency thereof.

## **DISCLAIMER**

**Portions of this document may be illegible  
in electronic image products. Images are  
produced from the best available original  
document.**

# Lattice-Matched Epitaxial GaInAsSb/GaSb Thermophotovoltaic Devices\*

C.A. Wang, H.K. Choi, G.W. Turner, D.L. Spears, and M.J. Manfra,

Lincoln Laboratory, Massachusetts Institute of Technology, Lexington, MA 02173-9108

G.W. Charache

Lockheed Martin, Inc., Schenectady, NY 12301

**Abstract.** The materials development of  $\text{Ga}_{1-x}\text{In}_x\text{As}_y\text{Sb}_{1-y}$  alloys for lattice-matched thermophotovoltaic (TPV) devices is reported. Epilayers with cutoff wavelength 2 - 2.4  $\mu\text{m}$  at room temperature and lattice-matched to GaSb substrates were grown by both low-pressure organometallic vapor phase epitaxy and molecular beam epitaxy. These layers exhibit high optical and structural quality. For demonstrating lattice-matched thermophotovoltaic (TPV) devices, p- and n- type doping studies were performed. Several TPV device structures were investigated, with variations in the base/emitter thicknesses and the incorporation of a high bandgap GaSb or AlGaAsSb window layer. Significant improvement in the external quantum efficiency is observed for devices with an AlGaAsSb window layer compared to those without one.

## INTRODUCTION

Recent developments of thermophotovoltaic (TPV) systems are based on thermal sources which operate in the temperature range 1100 - 1500K [1]. For high conversion efficiency, the cutoff wavelength of the photovoltaic cell should closely match the peak in emissive power of the thermal source, which for this temperature range corresponds to 1.9 - 2.6  $\mu\text{m}$ . Consequently, optimized cells

\* This work was sponsored by the Department of Energy under AF contract No. F19628-95-C-0002. The opinions, interpretations, conclusions and recommendations are those of the author and are not necessarily endorsed by the United States Air Force.

will be based on low-bandgap semiconductor materials. For example, InGaAs grown on InP substrates has been pursued [2,3]. However, the alloy composition that satisfies this wavelength range is lattice mismatched to the InP substrate, and defect filtering schemes must be incorporated to reduce crystalline defects. In spite of this limitation, TPV devices have exhibited external quantum efficiency (QE) as high as 50% at 2  $\mu\text{m}$  [3].

An alternative low-bandgap materials system is the  $\text{Ga}_{1-x}\text{In}_x\text{As}_y\text{Sb}_{1-y}$  quaternary alloy which has the advantage of being lattice matched to either GaSb or InAs substrates. The energy gap is dependent primarily on the In content, while As determines the lattice matching. Growth on GaSb substrates is preferred over InAs substrates due to thermodynamic considerations [4], electronic band structure[5], and mechanical stability [6]. Thermodynamically stable alloys with a cutoff wavelength of 2.39  $\mu\text{m}$  have been grown on GaSb by liquid phase epitaxy (LPE) [7]. Therefore, the  $\text{Ga}_{1-x}\text{In}_x\text{As}_{1-y}\text{Sb}_y$  alloys are of particular interest for TPV systems. Recently, GaInAsSb TPV devices grown by LPE and molecular beam epitaxy (MBE) have been demonstrated, and external QE exceeding 40% at 2  $\mu\text{m}$  has been obtained [6,8-9].

In this paper, we report the growth of  $\text{Ga}_{1-x}\text{In}_x\text{As}_y\text{Sb}_{1-y}$  alloys lattice matched to GaSb substrates by both organometallic vapor phase epitaxy (OMVPE) and MBE. Doping studies were performed, and the electrical, optical, and structural properties of these alloys grown using the different techniques are presented and compared. P-on-n  $\text{Ga}_{1-x}\text{In}_x\text{As}_y\text{Sb}_{1-y}$  devices were grown on GaSb substrates and evaluated. The effects of base/emitter thickness, surface passivation layer, and higher bandgap AlGaAsSb window layers on the quantum efficiency are presented.

## EPITAXIAL GROWTH AND CHARACTERIZATION

For OMVPE growth,  $\text{Ga}_{1-x}\text{In}_x\text{As}_y\text{Sb}_{1-y}$  epilayers were grown on (100) Te-doped GaSb or semi-insulating (SI) GaAs substrates misoriented 2° toward (110) or 6° toward (111)B. A vertical rotating-disk reactor with H<sub>2</sub> carrier gas at a flow rate of 10 slpm and reactor pressure of 150 Torr was used [10]. All organometallic sources including solution trimethylindium (TMIn),

triethylgallium (TEGa), tertiarybutylarsine (TBAs), and trimethylantimony (TMSb) were used with diethyltellurium (DETe) (50 ppm in H<sub>2</sub>) and dimethylzinc (DMZn) (1000 ppm in H<sub>2</sub>) as n- and p-type doping sources, respectively [11]. The total group III mole fraction was typically 3.5 to 4 x 10<sup>-4</sup> which resulted in a growth rate of ~2.7 μm/h. The V/III ratio was typically 1.1 - 1.3. The growth temperature ranged from 525 - 575°C. AlGaAsSb lattice-matched to GaSb substrates was grown with tritertiarybutylaluminum (TTBAI), TEGa, TBAs, and TMSb as previously described [12].

For MBE growth, epilayers were grown on (100) Te-doped GaSb or SI GaAs substrates in a solid-source EPI Gen II system. Conventional effusion cells were used to provide Ga, In, and Sb<sub>4</sub> fluxes, and a valved As cracker to provide As<sub>2</sub> as described previously [13]. The growth temperature was 500 to 510°C, and the growth rate was ~ 1 μm/h. Be was used as the p-type dopant, and GaTe as the n-type dopant.

The surface morphology was examined using Nomarski contrast microscopy. Double-crystal x-ray diffraction (DCXD) was used to measure the degree of lattice mismatch to GaSb substrates. Photoluminescence (PL) was measured at 4 and 300K using a cooled PbS detector. Electrical properties were obtained from Hall measurements based on the van der Pauw method. The composition of epilayers was determined from DCXD splitting, the peak emission in PL spectra, and the energy gap dependence on composition based on the binary bandgaps [14]:

$$E(x,y) = 0.726 - 0.961x - 0.501y + 0.08xy + 0.415x^2 + 1.2y^2 + 0.021x^2y - 0.62xy^2,$$

where  $y = 0.867x/(1 - 0.048x)$ , the condition for lattice matching to GaSb.

## GROWTH RESULTS

For OMVPE growth, the sensitivity of As incorporation (which controls the lattice matching on GaSb substrates) in Ga<sub>1-x</sub>In<sub>x</sub>As<sub>y</sub>Sb<sub>1-y</sub> (x ~ 0.13), was established by growing epilayers with various TBAs vapor phase concentration ratios,  $y_V = [TBAs]/([TBAs]+[TMSb])$ . The results, Figure 1, show that the lattice mismatch varies linearly with little deviation as a function of  $y_V$ ,

indicating that TBAs provides excellent controllability of lattice-matching conditions. Similar control of lattice matching was obtained for epilayers grown by MBE.

The surface morphology of lattice-matched GaInAsSb epilayers grown by OMVPE on (100) substrates with a 2° toward (110) misorientation was mirror-like to the eye, but for  $x > 0.1$ , exhibited a slight texture under Nomarski contrast. For epilayers grown on substrates with a 6° toward (111)B misorientation, the surface was mirror smooth. The morphology was mirror smooth for all MBE-grown epilayers. Cross-hatching was observed for all layers with a lattice mismatch  $> 5 \times 10^{-3}$ . Figure 2 shows the DCXD scan for a 2- $\mu\text{m}$ -thick  $\text{Ga}_{0.9}\text{In}_{0.1}\text{As}_{0.08}\text{Sb}_{0.92}$  layer. A narrow full width at half-maximum (FWHM) of 21 arc sec, which is comparable to 22 arc sec for the GaSb substrate, indicates the excellent structural quality of this layer. The x-ray splitting of 39 arc sec corresponds to a lattice mismatch of  $3 \times 10^{-4}$ . For lattice-matched epilayers, the DCXD scans are similar whether the layers are grown by OMVPE or MBE.

The optical quality of  $\text{Ga}_{1-x}\text{In}_x\text{As}_y\text{Sb}_{1-y}$  epilayers was evaluated by comparing the FWHM of PL spectra measured at 4K. Figure 3 summarizes the results for epilayers grown by OMVPE and MBE. The composition of epilayers was varied to cover the 300K energy range 0.55 - 0.72 eV, corresponding to 2.4 - 1.9  $\mu\text{m}$ . In general, the FWHM values are comparable for layers grown by OMVPE and MBE for 4K PL peak energy  $E_{\text{pk}} > 0.58$  eV. For lower  $E_{\text{pk}}$ , FWHM values are slightly larger for layers grown by OMVPE. Also shown for comparison are data for layers grown by LPE [15] and OMVPE [16].

The electrical properties were measured at 300K for nominally undoped  $\text{Ga}_{0.87}\text{In}_{0.13}\text{As}_{0.12}\text{Sb}_{0.88}$  layers grown on SI GaAs substrates. This composition corresponds to a cutoff wavelength of 2.2  $\mu\text{m}$  at 300K. Since the lattice mismatch between  $\text{Ga}_{1-x}\text{In}_x\text{As}_y\text{Sb}_y$  (lattice matched to GaSb) and GaAs is 8%, growth was first initiated with a GaSb buffer layer. For layers grown by OMVPE at 550°C, nominally undoped epilayers are p type with a typical hole concentration of  $5 - 8 \times 10^{15} \text{ cm}^{-3}$  and hole mobility 450 - 580  $\text{cm}^2/\text{V}\cdot\text{s}$ . Nominally undoped GaInAsSb layers grown by MBE are p type with a hole concentration of  $2 \times 10^{16} \text{ cm}^{-3}$  and mobility of  $\sim 300 \text{ cm}^2/\text{V}\cdot\text{s}$ .

The 300K electrical properties of n- and p-doped  $\text{Ga}_{0.87}\text{In}_{0.13}\text{As}_{0.12}\text{Sb}_{0.88}$  layers grown by OMVPE and MBE are summarized in Figures 4 and 5, respectively. Although the results for MBE-grown layers are somewhat limited, similar electrical characteristics are observed. For OMVPE layers, the electron concentration ranged from  $2.3 \times 10^{17}$  to  $2.3 \times 10^{18} \text{ cm}^{-3}$ , with corresponding mobility values of 5208 and 2084  $\text{cm}^2/\text{V}\cdot\text{s}$ , respectively. The hole concentration ranged from  $4.4 \times 10^{16}$  to  $1.7 \times 10^{18} \text{ cm}^{-3}$  with corresponding mobility values of 419 and 180  $\text{cm}^2/\text{V}\cdot\text{s}$ , respectively.

## DEVICE STRUCTURES AND FABRICATION

Several different TPV structures were grown for comparison. The basic structure consists of an n-GaInAsSb base layer and p-GaInAsSb emitter layer grown on a GaSb substrate. Variations to the structure included a variation in base/emitter layer thicknesses and incorporation of an AlGaAsSb/GaSb window layer. Device structures grown by OMVPE were on (100) GaSb substrates with either  $2^\circ$  toward (110) or  $6^\circ$  toward (111)B misorientation, while structures grown by MBE were on exactly (100) GaSb substrates. Table 1 summarizes the device structure, substrate orientation, 300K PL peak emission, and lattice mismatch  $\Delta a/a$ . The doping level of the p-GaInAsSb emitter layer was designed at  $\sim 2 \times 10^{17} \text{ cm}^{-3}$ , since our earlier studies on test structures indicated that for structures with  $p \leq 2 \times 10^{17} \text{ cm}^{-3}$ , the diode ideality factor ranged from 1.1 - 1.3 in the current density of 0.01 - 1  $\text{A}/\text{cm}^2$ . An increase in the ideality factor was observed for diodes fabricated from structures with higher hole concentrations, which may be related to tunneling [8].

Mesa diodes, 0.5 and 1  $\text{cm}^2$ , were fabricated by a conventional photolithographic process. A single 1-mm-wide central busbar connected to 10- $\mu\text{m}$  wide grid lines spaced 100  $\mu\text{m}$  apart was used to make electrical contact to the front surface. Ohmic contacts to p- and n-GaSb were formed by depositing Ti/Pt/Au and Au/Sn/Ti/Pt/Au, respectively, and alloying at 300°C. Mesas were formed by wet chemical etching to a depth of 5  $\mu\text{m}$ . No anti-reflection coatings were deposited on these test devices.

## DEVICE RESULTS

The external quantum efficiency (QE) as a function of wavelength for devices OM-379, OM-459, OM-462, and OM-463 are shown in Figure 6. The value of  $\Delta a/a$  of these structures is less than  $2 \times 10^{-3}$ . The highest QE near the bandedge is observed for OM-463 with a 3- $\mu\text{m}$ -thick emitter layer/1- $\mu\text{m}$ -thick base layer, which results because of the higher minority carrier diffusion length in p-type GaInAsSb compared to n-type GaInAsSb. However, at shorter wavelengths, the QE of OM-463 is lower than OM-462 which consists of 1- $\mu\text{m}$ -thick emitter layer/3- $\mu\text{m}$ -thick base layer. Since carriers are predominantly generated in the base layer for OM-462, this result suggests that these GaInAsSb devices are highly susceptible to surface recombination. The highest QE at wavelengths below 1.6  $\mu\text{m}$  is measured for OM-379 which has a GaSb window layer. In general, the performance of devices grown on (100) 2° toward (110) substrates are inferior to those grown on (100) 6° toward (111)B substrates. The QE of TPV devices grown by MBE (3- $\mu\text{m}$ -thick emitter layer/1- $\mu\text{m}$ -thick base layer) is similar to the results measured for OMVPE-grown devices.

Figure 7 shows the QE as a function of wavelength for OM-544 that consists of a 3- $\mu\text{m}$ -thick emitter layer, 1- $\mu\text{m}$ -thick base layer, and lattice-matched Al<sub>0.25</sub>Ga<sub>0.75</sub>As<sub>0.02</sub>Sb<sub>0.98</sub>/GaSb window layer. Higher bandgap window layers are often incorporated to improve the performance GaAs and InP solar cells [17]. For OM-544 with  $\Delta a/a < 1 \times 10^{-3}$ , the QE is nearly 60% over the whole wavelength range from 1.2 - 2.0  $\mu\text{m}$ , which is dramatically higher than devices shown in Figure 6 without the AlGaAsSb window layer, higher than has been previously reported for GaInAsSb/GaSb TPV devices [6,8-9], and approaching the ~70% limit for uncoated devices. Compared to OM-544, the QE is slightly lower by about 5% for OM-543 with  $\Delta a/a = 2.5 \times 10^{-3}$  and lowest for OM-542 with  $\Delta a/a = 5 \times 10^{-3}$ , indicating that structural defects affect the performance of these devices.

The 300K photoluminescence spectra of TPV structures with and without the AlGaAsSb window layer are shown in Figure 8. The PL efficiency is more than 5 times higher for the structure with the window layer. Since carriers are generated near the surface in these PL experiments (excitation source is 647 nm),

these results indicate that the AlGaAsSb is especially effective in passivating the surface of the underlying GaInAsSb and effectively reduces the surface recombination velocity. Furthermore, standard calculations [18] of external QE suggest that the surface recombination velocity may be reduced by several orders of magnitude with the AlGaAsSb window layer and that the minority electron diffusion length in our lattice-matched GaInAsSb is about 5  $\mu\text{m}$ . The QE is comparable to lattice-mismatched InGaAs/InP devices, which had a maximum QE of 65% at 1.2  $\mu\text{m}$  and dropped off to 53% at 2.0  $\mu\text{m}$  [3]. Further characterization of GaInAsSb/AlGaAsSb/GaSb devices should be performed to assess the potential of this materials system for TPV systems.

## CONCLUSIONS

High-quality GaInAsSb epilayers were grown lattice matched to GaSb substrates by OMVPE and MBE. The use of a higher bandgap AlGaAsSb window layer is particularly effective in increasing the external QE by reducing surface recombination velocity, and results in overall improved performance especially at shorter wavelengths. External QE over 55% between 1.2 - 2  $\mu\text{m}$  has been measured. The present results suggest that GaInAsSb materials system is promising for high performance TPV systems with source temperatures operating 1100 - 1500K.

## ACKNOWLEDGMENTS

The authors gratefully acknowledge D.R. Calawa, J.W. Chludzinski, M.K. Connors, C.D. Hoyt, P.M. Nitishin, D.C. Oakley, R.J. Poillucci, and V. Todman-Bams for technical assistance, K.J. Challberg for manuscript editing, and B-Y. Tsaur for continued support and encouragement.

## REFERENCES

1. J.P. Benner, T.J. Coutts, and D.S. Ginley, *2nd NREL Conference on the Thermophotovoltaic Generation of Electricity*, AIP Conf. Proc. **358**, Woodbury, NY, 1995.
2. Wanlass, M.W., Ward, J.S., Emery, K.A., Al-Jassim, M.M., Jones, K.M. and Coutts, T.J., "Ga<sub>x</sub>In<sub>1-x</sub>As thermophotovoltaic converters," *Solar Energy Mater. and Solar Cells* **41/42**, 405-417 (1996).
3. Wojtczuk, S., Colter, P., Charache, G., and Campbell, B., "Production data on 0.55 eV InGaAs thermophotovoltaic cells," *Proc. 25th IEEE Photovoltaic Specialist Conference*, p. 77-80 (1996).
4. Cherng, M.J., Jen, H.R., Larsen, C.A., Stringfellow, G.B., Lundt, H. and Taylor, P.C., "MOVPE growth of GaInAsSb," *J. Cryst. Growth* **77**, 408-417 (1986).
5. Milnes, A.G. and Polyakov, A.Y., "Indium arsenide: a semiconductor for high speed and electro-optical devices," *Mater. Sci. and Engin.*, **B18**, 237-259 (1993).
6. Uppal, P.N., Charache, G., Baldasaro, P.F., Campbell, B.C., Loughin, S., Svensson, S., and Gill, D., "MBE growth of GaInAsSb p/n junction diodes for thermophotovoltaic applications," *to appear J. Cryst. Growth*.
7. Tournie, E., Pitard, F., and Joullie, A., "High temperature liquid phase epitaxy of (100) oriented GaInAsSb near the miscibility gap boundary," *J. Cryst. Growth* **104**, 683-694 (1990).
8. Charache, G.W., Egley, J.L., Danielson, L.R., DePoy, D.M., Baldasaro, P.F., Campbell, B.C., Hui, S., Frass, L.M., Wojtczuk, S.J., "Current status of low-temperature radiator thermophotovoltaic devices," *Proc. 25th IEEE Photovoltaic Specialist Conference*, p. 137-140 (1996).
9. Shellenbarger, Z.A., Mauk, M.G., DiNetta, L.C. and Charache, G.W., "Recent progress in InGaAsSb/GaSb TPV devices," *Proc. 25th IEEE Photovoltaic Specialist Conference*, p. 81-84 (1996).
10. Wang, C.A., Patnaik, S., Caunt, J.W., and Brown, R.A., "Growth characteristics of a vertical rotating-disk OMVPE reactor," *J. Cryst. Gr.* **93**, 228-234 (1988).
11. Wang, C.A. and Choi, H.K., "OMVPE Growth of GaInAsSb/AlGaAsSb for Quantum-Well Diode Lasers," *to appear J. Electron. Mater.*
12. Wang, C.A., "Organometallic Vapor Phase Epitaxial Growth of AlSb-based alloys," *J. Cryst. Growth* **170**, 725-731 (1997).

13. Turner, G.W., Choi, H.K., Calawa, D.R., Pantano, J.V., and Chludzinski, J.W., "Molecular-beam growth of high-performance midinfrared diode lasers," *J. Vac. Sci. Technol. B* **12**, 1266–1268 (1994).
14. DeWinter, J.C., Pollock, M.A., Srivastava, A.K., and Zyskind, J.L., "Liquid phase epitaxial  $\text{Ga}_{1-x}\text{In}_x\text{As}_y\text{Sb}_{1-y}$  lattice-matched to (100) GaSb over the 1.71 to 2.33  $\mu\text{m}$  wavelength range," *J. Electron. Mater.* **14**, 729–747 (1985).
15. Tournie, E., Lazzari, J.-L., Pitard, F., Alibert, C., Joullie, A., and Lambert, B., "2.5  $\mu\text{m}$  GaInAsSb lattice-matched to GaSb by liquid phase epitaxy," *J. Appl. Phys.* **68**, 5936–5938 (1990).
16. Sopanen, M., Koljonen, T., Lipsanen, H., and Tuomi, T., "Growth of GaInAsSb using tertiarybutylarsine as arsenic source," *J. Cryst. Growth* **145**, 492–497 (1994).
17. Hovel, H.J., *Solar Cells*, Semiconductors and Semimetals, Vol. 11, Academic Press, NY, 1975.
18. Moller, H.J., *Semiconductors for Solar Cells*, Artech House, Inc., Boston, 1993.

## FIGURE CAPTIONS

Figure 1 Dependence of lattice mismatch of GaInAsSb epilayers grown at 575°C by OMVPE on GaSb substrates as function of TBAs gas phase concentration.

Figure 2 Double-crystal x-ray diffraction scan of  $\text{Ga}_{0.9}\text{In}_{0.1}\text{As}_{0.08}\text{Sb}_{0.92}$  grown at 575°C on GaSb by OMVPE.

Figure 3 Full width at half-maximum of photoluminescence spectra measured at 4K of GaInAsSb layers grown on GaSb substrates by OMVPE and MBE.

Figure 4 Electrical properties measured at 300K of n- $\text{Ga}_{0.87}\text{In}_{0.13}\text{As}_{0.12}\text{Sb}_{0.88}$  grown by OMVPE and MBE.

Figure 5 Electrical properties measured at 300K of p- $\text{Ga}_{0.87}\text{In}_{0.13}\text{As}_{0.12}\text{Sb}_{0.88}$  grown by OMVPE and MBE.

Figure 6 External quantum efficiency of TPV devices described in Table 1.

Figure 7 External quantum efficiency of TPV devices with AlGaAsSb window layer.

Figure 8 Photoluminescence spectra of TPV devices with and without AlGaAsSb window layer.

Table 1

Run	n-GaInAsSb(μm)	p-GaInAsSb(μm)	p-AlGaAsSb(μm)	p-GaSb(μm)	orientation	300K PL peak emission (μm)	Δa/a(×10 <sup>-3</sup> )
OM-379	3	0.2	0	0.05	(100) 2(110)	2.15	0
OM-459	3	1	0	0	(100) 2(110)	2.24	2
OM-462	3	1	0	0	(100) 6(111)B	2.24	1
OM-463	1	3	0	0	(100) 6(111)B	2.24	1.5
OM-542	1	3	0.1	0.025	(100) 6(111)B	2.26	5
OM-543	1	3	0.1	0.025	(100) 6(111)B	2.26	2.5
OM-544	1	3	0.1	0.025	(100) 6(111)B	2.26	0.6
MBE-041	1	3	0	0	(100)-	2.14	1

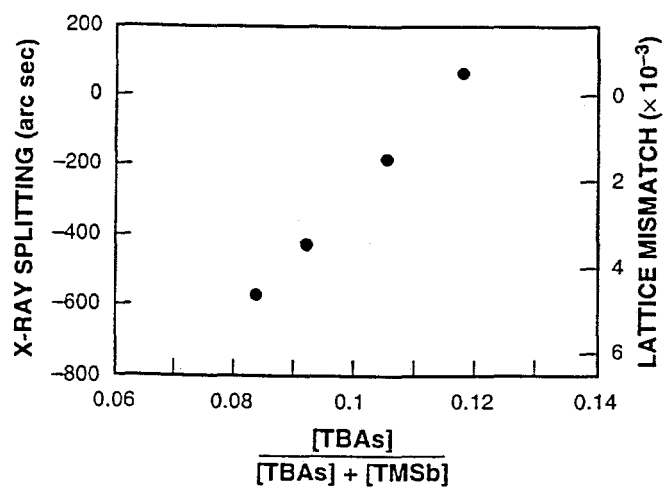


Figure 1

294395-8

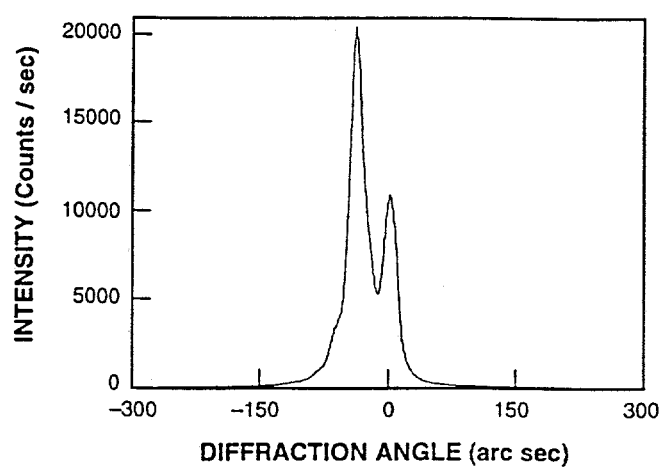


Figure 2

294395-1

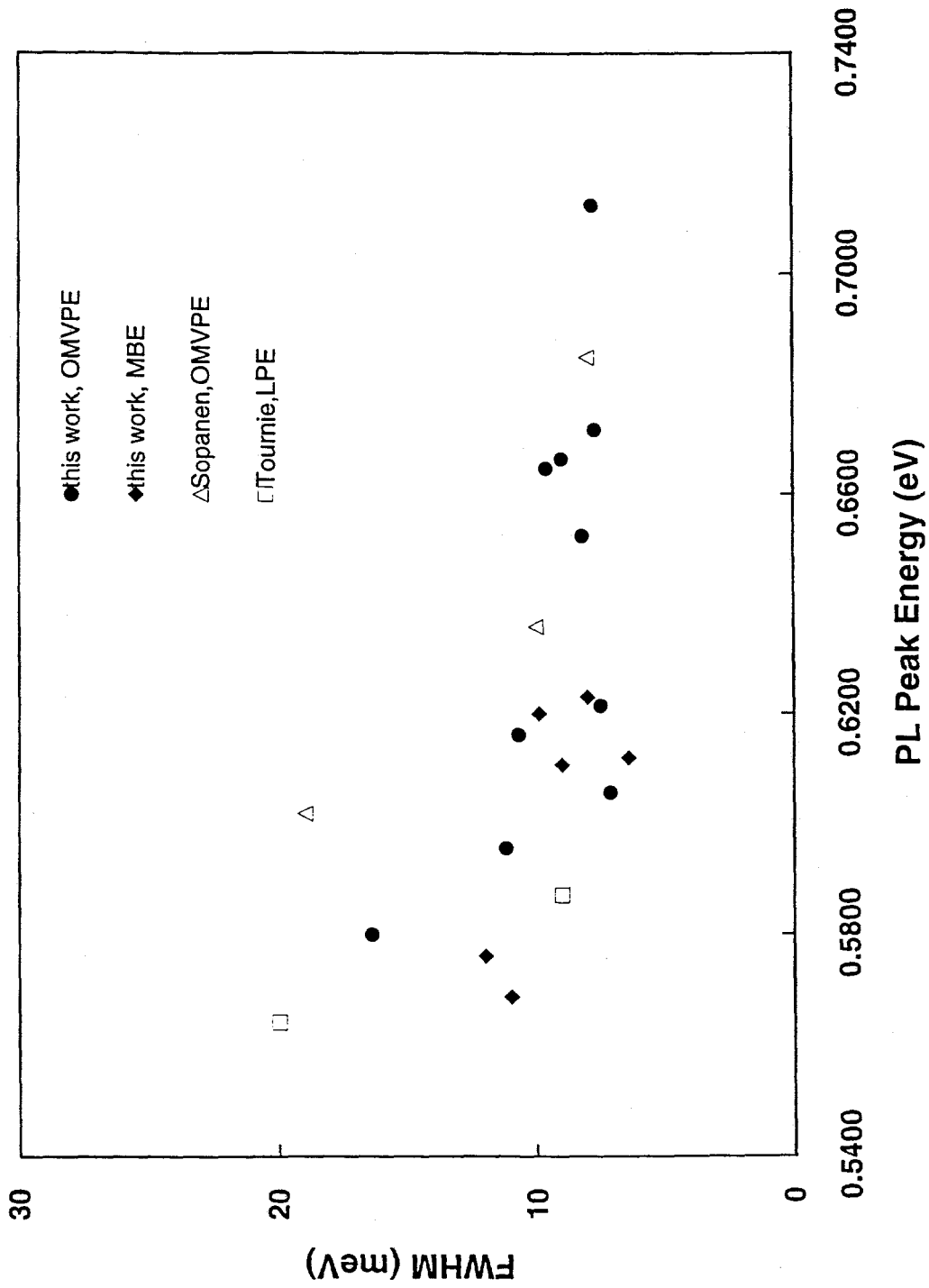


Figure 3

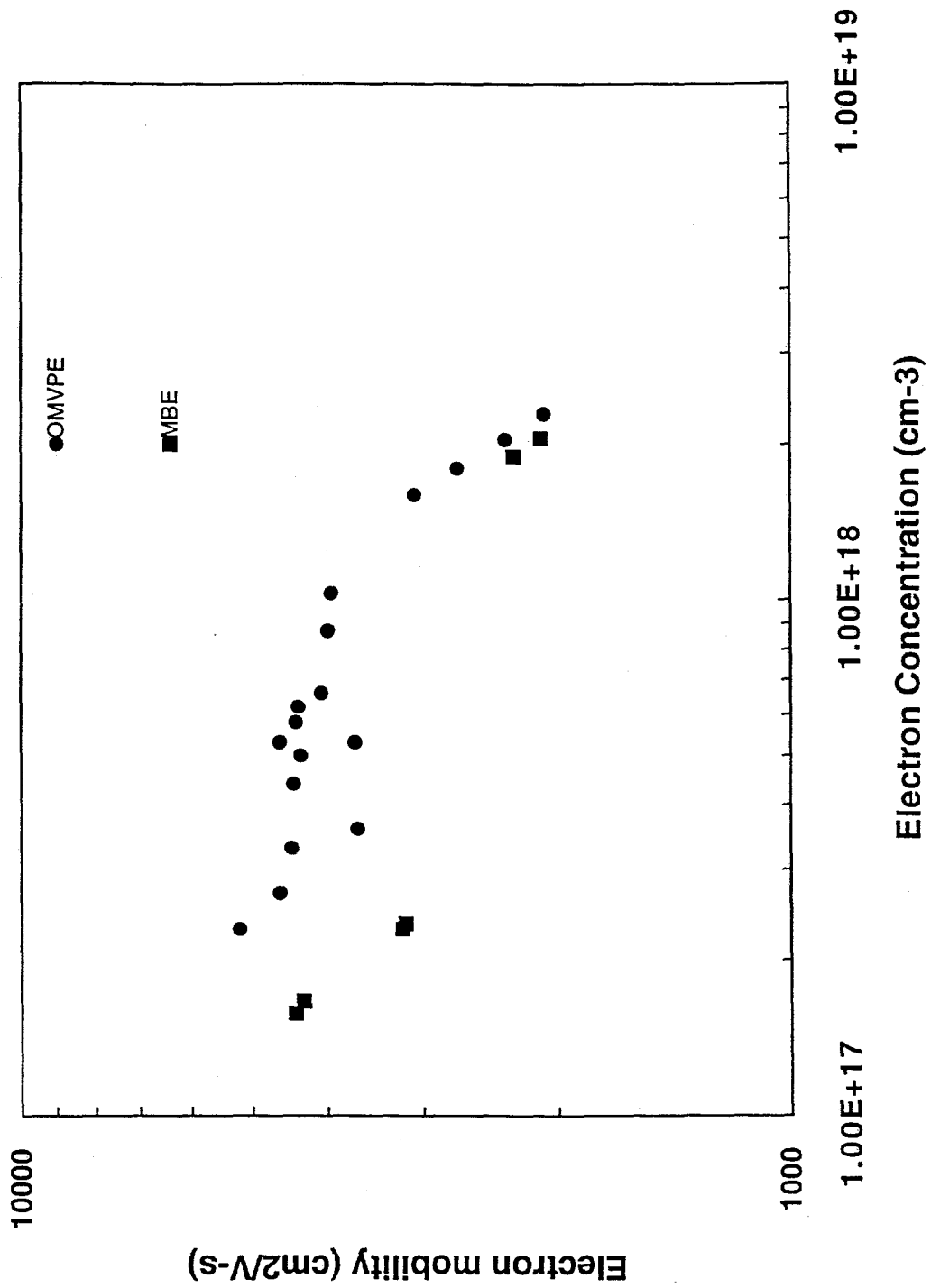


Figure 4

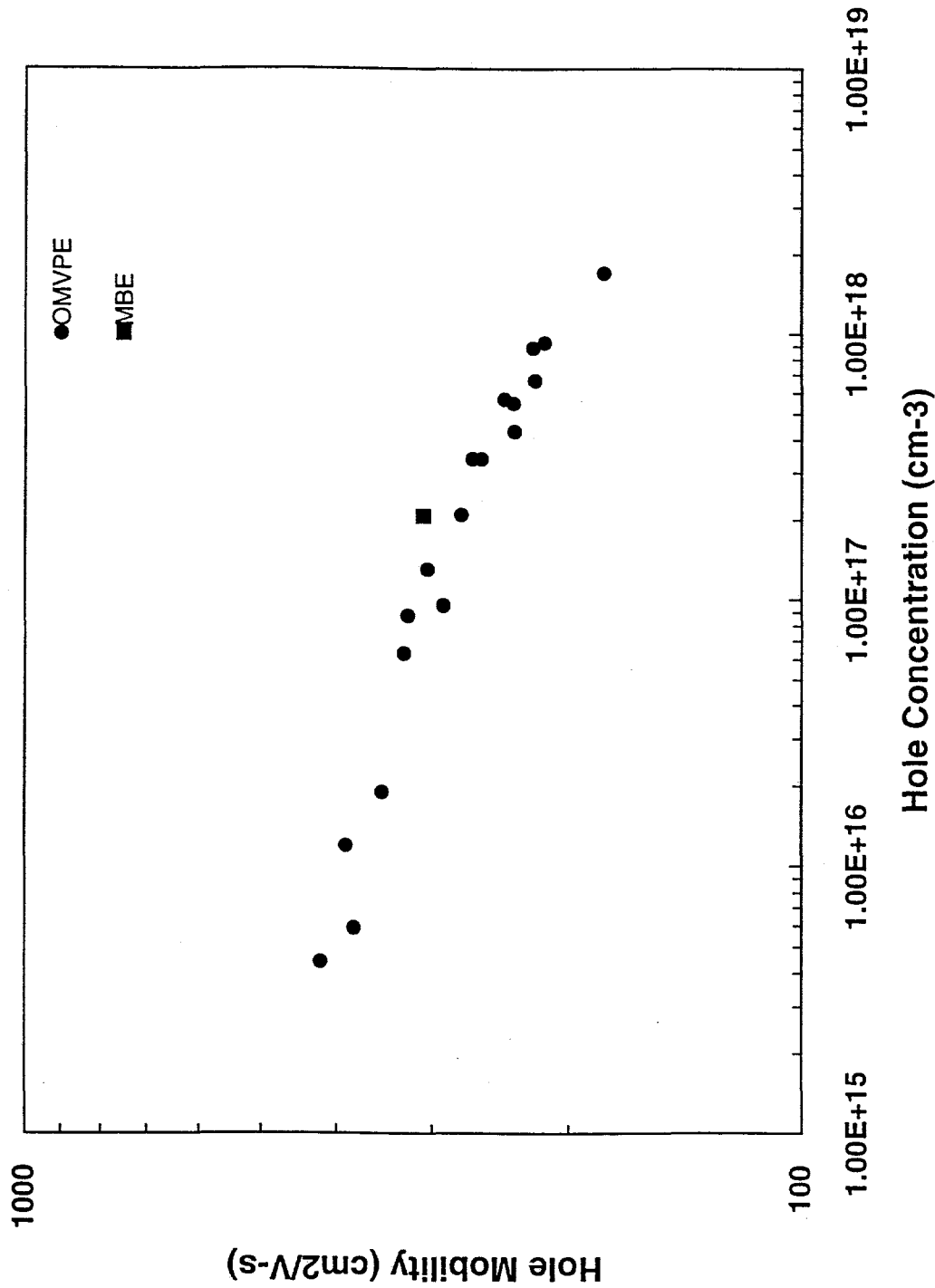


Figure 5

### Quantum Efficiency of Lincoln Laboratory Cells

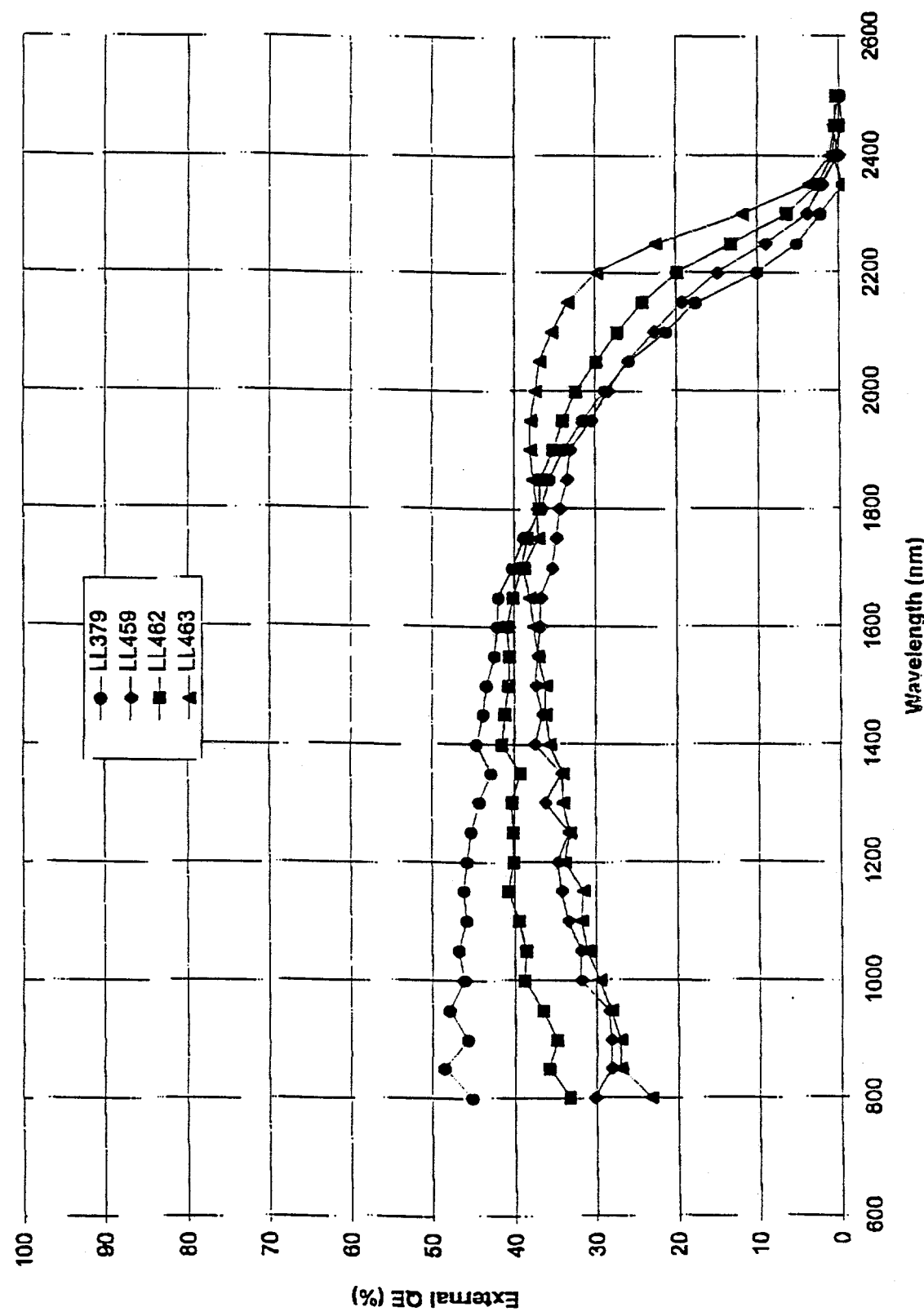


Figure 6

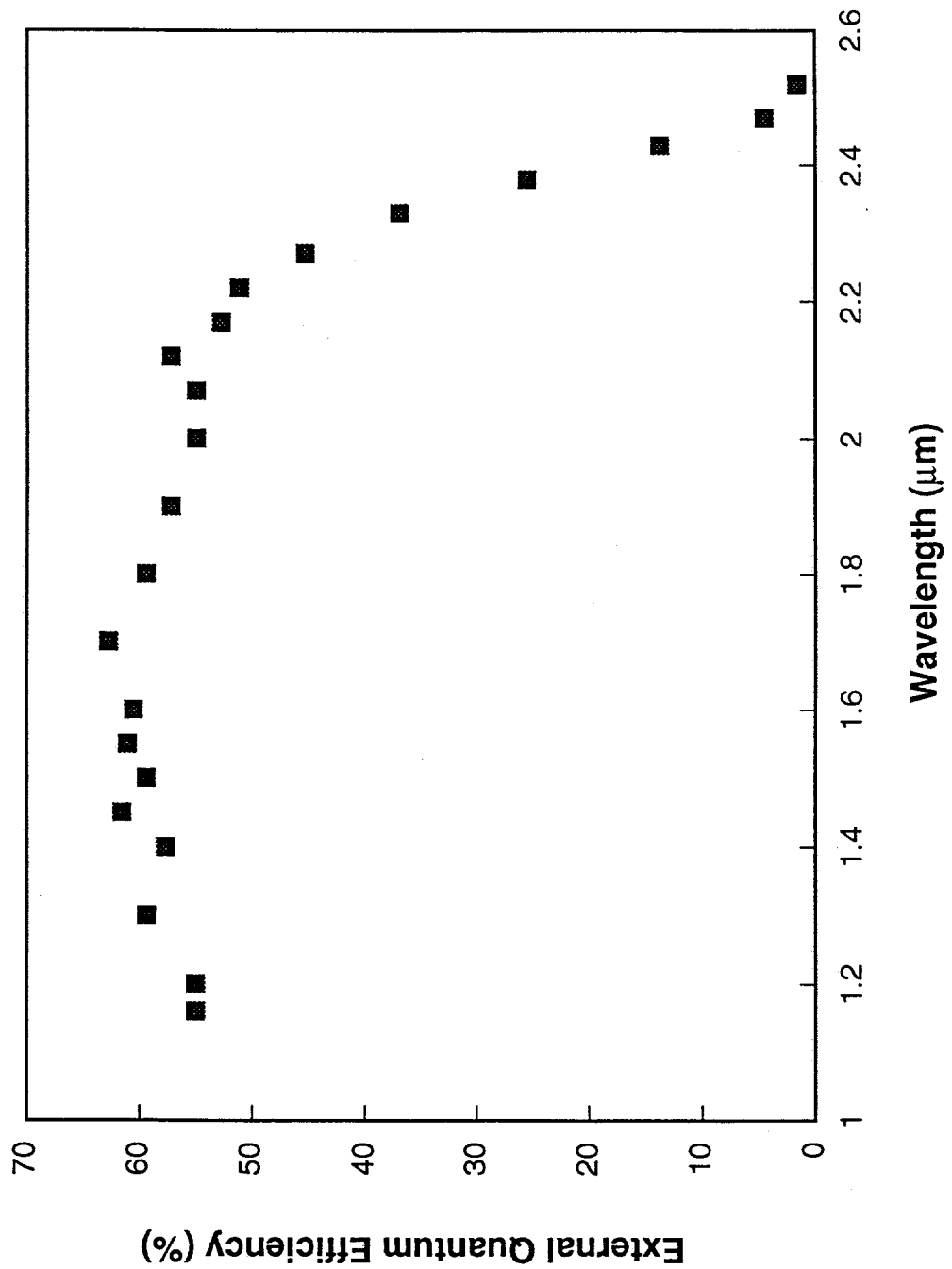


Figure 7

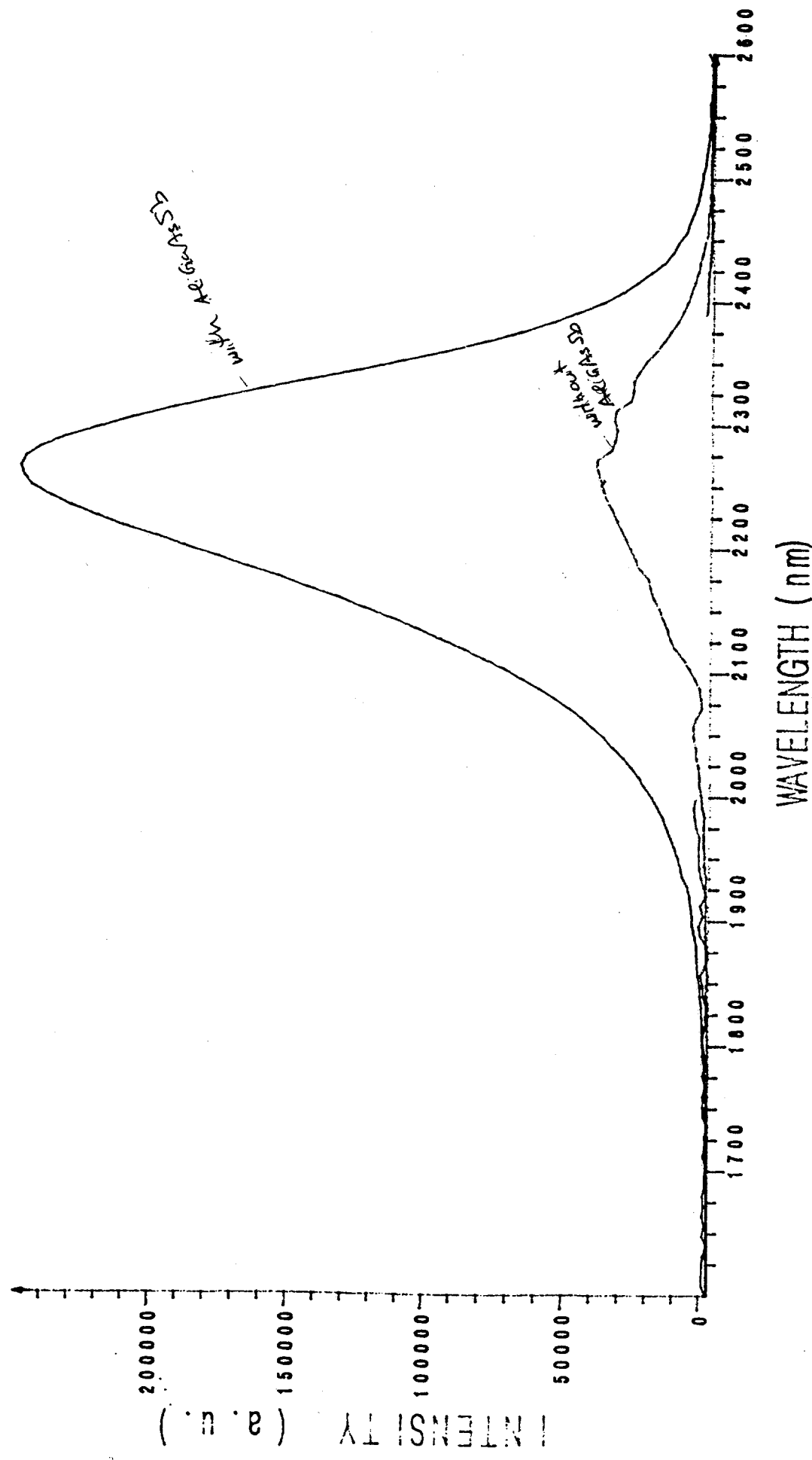


Figure 8